Article

A Gadolinium Chelate for Detection of β-Glucuronidase: A Self-Immolative Approach

Joseph A. Duimstra, Frank J. Femia, and Thomas J. Meade

J. Am. Chem. Soc., **2005**, 127 (37), 12847-12855• DOI: 10.1021/ja042162r • Publication Date (Web): 23 August 2005

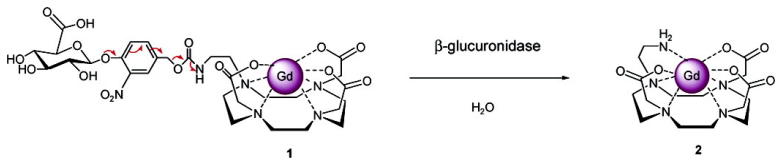

More About This Article

Additional resources and features associated with this article are available within the HTML version:

- Supporting Information
- Links to the 14 articles that cite this article, as of the time of this article download
- Access to high resolution figures
- Links to articles and content related to this article
- Copyright permission to reproduce figures and/or text from this article

View the Full Text HTML

J|A|C|S
ARTICLES
Published on Web 08/23/2005

A Gadolinium Chelate for Detection of β-Glucuronidase: A Self-Immolative Approach

Joseph A. Duimstra,[1] Frank J. Femia,[2] and Thomas J. Meade*

Contribution from the Departments of Chemistry, Biochemistry and Molecular and Cell Biology, Neurobiology and Physiology, and Radiology, Northwestern University, Evanston, Illinois 60201

Received December 29, 2004; E-mail: tmeade@northwestern.edu

Abstract: New classes of physiologically responsive magnetic resonance (MR) contrast agents are being developed that are activated by enzymes, secondary messengers, pH, and temperature. To this end, we have prepared a new class of enzyme-activated MR contrast agents using a self-immolative mechanism and investigated the properties of these agents using novel in vitro assays. We have synthesized in nine steps a Gd(III) agent **1** that is activated by the oncologically significant β-glucuronidase. **1** consists of Gd(III)DO3A (DO3A = 1,4,7-tricarboxymethylene-1,4,7,10-tetraazacyclododecane) bearing a pendant β-glucuronic acid moiety connected by a self-immolative linker to the macrocycle. LC−MS analysis reveals that **1** is enzymatically processed as predicted by bovine liver β-glucuronidase, generating 2-aminoethyl-GdDO3A, **2**. Compound **2** was prepared independently in a four-step synthetic procedure. Complex **1** displays a decrease in relaxivity upon titration with bicarbonate anion. The relaxivity increases when **1** is converted to **2** in a buffer mimicking in vivo anion concentrations (Parker, D. In *Crown Compounds: Towards Future Applications*; Cooper, S. R., Ed.; VCH: New York, 1992; pp 51−67) by 17%, while the relaxivity decreases by 27% for the same experiment in human blood serum. Hydrolytic kinetics catalyzed by bovine liver β-glucuronidase at interstitial pH = 7.4 fit the Michaelis−Menten model with $k_{cat}/K_m = 74.9 \pm 10.9$ M^{-1} s^{-1}. Monitoring of bulk water proton T_1 during incubation with enzyme shows an increase in T_1 that mirrors results obtained through the relaxivity measurements of compounds **1** and **2**.

Introduction

Cancer is a leading cause of death in developed nations, prompting extensive research into the myriad aspects of this heterogeneous disease. The ability to noninvasively detect a small number of cells at the onset of metastatic growth presents a major challenge not only to clinicians but also to the experimental community. Potential exists for cancer detection through the in vivo, noninvasive visualization of cellular and biochemical events that has been gaining rapid momentum in the burgeoning field of molecular imaging.[4−8] Imaging constructs that function within the chemotherapeutic cancer prodrug paradigm are particularly attractive given the extensive research in the latter field.[9−13]

The application of β-glucuronide prodrugs in prodrug monotherapy (PMT) has yielded mixed results.[14,15] In PMT, β-glucuronic acid is liberated from the relatively nontoxic prodrug via endogenous extracellular β-glucuronidase, yielding the more potent chemotherapeutic. The drawbacks to this approach are that high enzyme levels are found only near necrotic tumor masses that have low perfusion and hence receive less prodrug, and that enzyme concentration is variable between individuals.[9,10] Further complicating matters is the short half-life of glucuronide-conjugated prodrugs, necessitating fast enzymatic conversion of the prodrug to its active form.[15] Antibody-directed enzyme prodrug therapy (ADEPT; a two-step approach) introduces exogenous enzyme via an antibody-targeting moiety and, in principle, should overcome the problems associated with PMT. ADEPT progress, initially curtailed by host immune response to the antibody−enzyme conjugate, has shown promise with the advent of antibodies engineered via phage display[16] and human-based fusion proteins.[17] Another potential avenue

(1) Division of Chemistry and Chemical Engineering, California Institute of Technology, Pasadena, CA 91125.
(2) Present address: Molecular Insight Pharmaceuticals Inc., Cambridge, MA 02142.
(3) Deleted in proof.
(4) *J. Magn. Reson. Imaging*, Special Issue: Molecular Imaging **2002**, *4*, 333−483.
(5) Li, K.; Pandit, S.; Guccione, S.; Bednarski, M. *Biomed. Microdev.* **2004**, *6*, 113−116.
(6) *J. Cell. Biochem.*, Supplement: Molecular Imaging **2002**, *87*, supplement 39, 1−248.
(7) Nordberg, A. *Lancet Neurol.* **2004**, *3*, 519−527.
(8) Choy, G.; Choyke, P.; Libutti, S. K. *Mol. Imaging* **2003**, *2*, 303−312.
(9) Rooseboom, M.; Commandeur, J. N. M.; Vermeulen, N. P. E. *Pharmacol. Rev.* **2004**, *56*, 53−102.
(10) Brusselbach, S. *Methods Mol. Med.* **2004**, *90*, 303−330.
(11) Papot, S.; Tranoy, I.; Tillequin, F.; Florent, J. C.; Gesson, J. P. *Curr. Med. Chem.: Anti-Cancer Agents* **2002**, *2*, 155−185.
(12) Xu, G.; McLeod, H. L. *Clin. Cancer Res.* **2001**, *7*, 3314−3324.
(13) Tietze, L. F.; Feuerstein, T. *Aust. J. Chem.* **2003**, *56*, 841−854.
(14) Bosslet, K.; Straub, R.; Blumrich, M.; Czech, J.; Gerken, M.; Sperker, B.; Kroemer, H. K.; Gesson, J.-P.; Koch, M.; Monneret, C. *Cancer Res.* **1998**, *58*, 1195−1201.
(15) Guerquin-Kern, J.-L.; Volk, A.; Chenu, E.; Lougerstay-Madec, R.; Monneret, C.; Florent, J.-C.; Carrez, D.; Croisy, A. *NMR Biomed.* **2000**, *13*, 306−310.
(16) Pedley, R. B.; Sharma, S. K.; Hawkins, R. E.; Chester, K. A. *Methods Mol. Med.* **2004**, *90*, 491−514.
(17) Biela, B. H.; Khawli, L. A.; Hu, P.; Epstein, A. L. *Can. Biother. Radiopharm.* **2003**, *18*, 339−353.

involves gene-directed enzyme prodrug therapy (GDEPT). Here, the diseased cells are transfected with DNA coding for the enzyme that is then produced by the cell and effects the prodrug cleavage. The cell surface display of β-glucuronidase has recently been reported as a candidate for GDEPT.[18]

The proven clinical capacity of magnetic resonance imaging (MRI) combined with the lack of ionizing radiation affords a valuable tool for in vivo, whole organism molecular imaging. Since the intrinsic contrast of MRI results from the physical properties and local environment of endogenous water, this technique has predominantly focused on anatomical structure. The quest for higher resolution and shorter acquisition times has spurred the development of agents that increase the observed contrast in MR images.[19,20] Much work has focused on increasing the effectiveness of small-molecule contrast agents based on Gd(III) chelates with particularly promising results derived from interactions with macromolecules.[21−23] While these compounds delineate anatomical structure, new agents that are biochemical and physiological reporters are being developed.[24−29] Barriers to the development of new generations of biologically responsive agents include the lack of adequate in vitro assays to determine efficacy, enzyme kinetics, delivery, and inherent contrast.

Here, we report a new class of MR contrast agents that uses a self-immolative mechanism for activation in the presence of an enzyme. The prototype of this class is a Gd(III) agent designed to function within the β-glucuronidase prodrug family. This agent's effect on water proton T_1 relaxation is modulated by hydrolysis of β-glucuronic acid (Scheme 1). Previous studies using β-galactosidase-sensitive EGad and EGadMe revealed that the in vitro behavior of these agents does not reflect their in vivo activity.[24,25] Therefore, we have developed and exploited in vitro assays using compounds **1** and **2** to gain insight into factors affecting in vivo activity.

Experimental Section

General Methods. All reagents were used as purchased. 1,4,7,10-Tetraazacyclododecane (cyclen) was obtained from Strem. Prohance was purified from the clinically available sample from Bracco Inc. using HPLC. Bovine liver β-glucuronidase [EC 3.2.1.31] Sigma cat G 0251 (Type B-1), BSA fraction V Sigma cat A 3059, *p*-nitrophenyl-β-D-glucuronide, and male human blood serum Sigma cat H 1388 were procured from Sigma. Dry solvents, where indicated, were obtained from Aldrich as anhydrous Sure-Seal bottles. Water was purified using a Millipore Milli-Q Synthesis purifier. Sugar-containing compounds were visualized on silica TLC plates with CAM stain (1 g of $(NH_4)_4Ce(SO_4)_4$, 2.5 g of $(NH_4)_4Mo_2O_7$, 6 mL of concentrated H_2SO_4, 94 mL of water), while compounds containing unmetalated cyclen could be easily detected using a platinum stain (150 mg of K_2PtCl_6, 10 mL of 1 N HCl, 90 mL of water, 3 g of KI). NMR spectra were recorded on either a Varian Mercury 400 MHz or Varian Inova 500 MHz instrument. Peaks were referenced to an internal TMS standard. Infrared spectra were measured using a KBr plate on a Biorad FTS-60 FTIR spectrometer. Electrospray mass spectra were obtained via direct infusion of a methanolic solution of the compound of interest on a Varian 1200L single quadrupole mass spectrometer. Elemental analysis was performed by Desert Analytics (Tucson, AZ). ICP-MS were recorded on a VG Elemental PQ Excell spectrometer standardized with eight concentrations spanning the range of 0−50 ppb Gd(III). One part per billion In(III) was used as the internal standard for all runs. UV−visible spectroscopy was performed on a HP 8452A diode array spectrometer thermostated to 37 °C.

Scheme 1

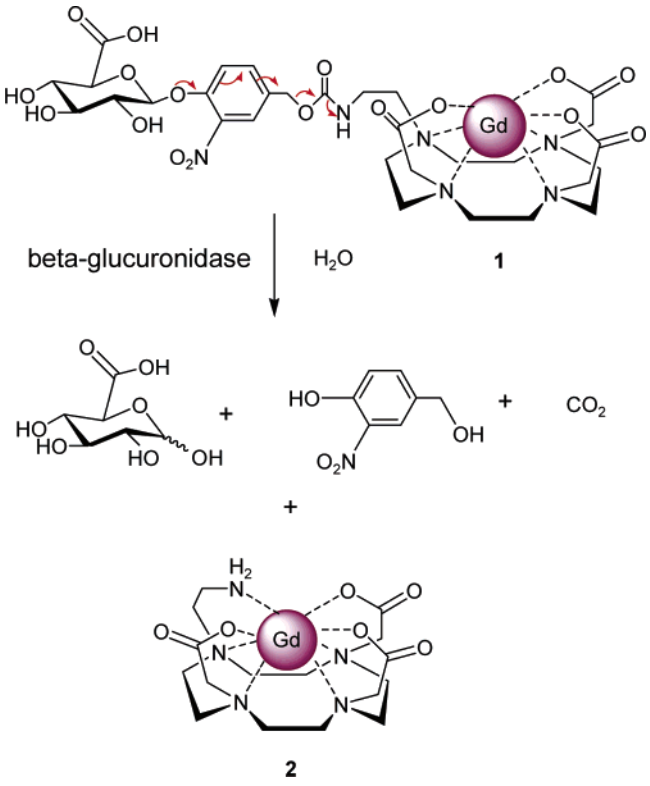

LC−MS. Analytical LC−MS was performed on a computer-controlled Varian Prostar system consisting of a 410 autosampler equipped with a 100 μL sample loop, two 210 pumps with 5 mL/min heads, a 363 fluorescence detector, a 330 photodiode array (PDA) detector, and a 1200L single quadrupole ESI-MS. All runs were executed with a 0.8 mL/min flow rate using a ThermoElectron 4.6 × 150 mm 5 μm Aquasil C18 column, with a 3:1 split directing one part to the MS and three parts to the series-connected light detectors. Mobile phase consisted of water (solvent A) and HPLC-grade acetonitrile (solvent B) except where noted. All injections were full-loop.

Preparative LC. The preparative system is a Varian Prostar. Two 210 pumps with 25 mL/min heads fed a 5 mL manual inject sample loop. Detection was performed after a 20:1 split by a two-channel 325 UV−visible detector and, on the low-flow leg, a HP 1046A fluorescence detector. The mobile phases were the same as in the LC−MS instrument. Preparative runs were typically 50−100 mg dissolved in water and run at 15 mL/min on a ThermoElectron 20 × 250 mm 5 μm Aquasil C18 column.

(18) Heine, D.; Muller, R.; Brusselbach, S. *Gene Therapy* **2001**, *8*, 1005−1010.
(19) Merbach, A. E.; Toth, E. *The Chemistry of Contrast Agents in Medical Magnetic Resonance Imaging*; John Wiley and Sons: West Sussex, New York, 2001.
(20) Caravan, P.; Ellison, J. J.; McMurry, T. J.; Lauffer, R. B. *Chem. Rev.* **1999**, *99*, 2293−2352.
(21) Caravan, P. et al. *J. Am. Chem. Soc.* **2002**, *124*, 3152−3162.
(22) Aime, S.; Botta, M.; Fasano, M.; Crich, S. G.; Terreno, E. *J. Biol. Inorg. Chem.* **1996**, *1*, 312−319.
(23) Doble, D. M. J.; Botta, M.; Wang, J.; Aime, S.; Barge, A.; Raymond, K. N. *J. Am. Chem. Soc.* **2001**, *123*, 10758−10759.
(24) Moats, R. A.; Fraser, S. E.; Meade, T. J. *Angew. Chem., Int. Ed. Engl.* **1997**, *36*, 726−728.
(25) Louie, A. Y.; Huber, M. M.; Ahrens, E. T.; Rothbacher, U.; Moats, R.; Jacobs, R. E.; Fraser, S. E.; Meade, T. J. *Nat. Biotechnol.* **2000**, *18*, 321−325.
(26) Alauddin, M. M.; Louie, A. Y.; Shahinian, A.; Meade, T. J.; Conti, P. S. *Nucl. Med. Biol.* **2003**, *30*, 261−265.
(27) Allen, M. J.; Meade, T. J. *Metal Ions Biol. Syst.* **2004**, *42*, 1−38.
(28) Morawski, A. M.; Winter, P. M.; Crowder, K. C.; Caruthers, S. D.; Fuhrhop, R. W.; Scott, M. J.; Robertson, J. D.; Abendschein, D. R.; Lanza, G. M.; Wickline, S. A. *Magn. Reson. Med.* **2004**, *51*, 480−486.
(29) Nivorozhkin, A. L.; Kolodziej, A. F.; Caravan, P.; Greenfield, M. T.; Lauffer, R. B.; McMurry, T. J. *Angew. Chem., Int. Ed.* **2001**, *40*, 2903−2906.

Methyl-1-(4-(2-(1-(1,4,7,10-tetraazacyclododecyl))ethylcarbamoyloxymethyl)-2-nitrophenyl)-β-D-glucopyronuronate (12). Cyclen (541 mg, 3.14 mmol) and **10** (640 mg, 1.26 mmol) were combined in 19 mL of DMSO, and the reaction was allowed to stir overnight. TLC analysis at this time (10% MeOH/CH_2Cl_2) indicated no unreacted sugar. The solvent was removed in vacuo, yielding a viscous yellow oil. The oil was dissolved in 7 mL of MeOH, and a pale yellow solid precipitated upon addition of 50 mL of Et_2O. Upon storage at −20 °C for 1 h, the hygroscopic solid was collected on a glass frit, washed with Et_2O (3 × 3 mL), and dried under vacuum, yielding 908 mg of solid. TLC (silica; 1:9:90 sat. KNO_3 (aq.):water:MeCN; Pt stain visualization) and ESI-MS showed very low intensity di- and trisubstituted side product peaks. The precipitation procedure removed excess free base cyclen; however, MS and ^{1}H NMR showed that the desired product was contaminated with cyclen hydrobromide salt. This mixture was used in the subsequent reaction without further purification.

Methyl-1-(4-(2-(1-(4,7,10-trisethylcarboxymethyl-(1,4,7,10-tetraazacyclododecyl)))ethylcarbamoyloxymethyl)-2-nitrophenyl)-β-D-glucopyronuronate (13). A quantity of 887 mg of the mixture containing **12** and 1.23 g of K_2CO_3 were suspended in 30 mL of acetone; 820 μL of α-bromoethylacetate was added, and the solution was allowed to stir at room temperature overnight. An additional 164 μL of α-bromoethylacetate and 210 mg K_2CO_3 were added after 24 h. At 48 h, the reaction mixture was filtered to remove solids and purified by flash chromatography (silica, 0−13.3% MeOH in CH_2Cl_2). The resulting solid was dissolved in acetone and filtered through a 0.2 μm PTFE filter to remove excess silica. This yielded 510 mg of **13**. Elemental bromine analysis indicated the presence of a mixture of free base and hydrobromide salt. ESI-MS and ^{1}H NMR showed no evidence of lactamization. ^{1}H NMR (500 MHz, CD_3OD): δ 1.25 (m, 9H, $COOCH_2CH_3$), 2.0−3.4 (br, 24H, cyclen H's, 2H-sugar, acetate CH_2), 3.52 (m, 4H), 3.64 (m, 1H), 3.76 (s, 3H, $COOCH_3$), 4.10 (d, 1H, J = 10 Hz), 4.12−4.24 (m, 6H, $COOCH_2CH_3$), 5.07 (s, 2H, benzylic CH_2), 5.21 (d, 1H, H-1, J = 7 Hz), 7.39 (d, ArH, J = 8 Hz), 7.60 (d, 1H, ArH, J = 8 Hz), 7.83 (s, 1H, ArH); ^{13}C NMR (126 MHz, CD_3OD) δ 14.64, 14.67, 38.73, 53.10, 55.99, 56.44, 56.88 (br), 62.61, 62.83, 66.01, 72.79, 74.46, 76.90, 77.25, 102.30, 118.81, 125.33, 133.50, 134.31, 142.19, 150.54, 159.14, 170.76, 175.57, 175.66 (br). ESI-MS m/z $(M + H)^+$ 859.2 (40%), $(M + Na)^+$ 881.2 (100%). Anal. Calcd for $C_{37}H_{58}N_6O_{17}$·acetone·2.5H_2O·0.75HBr: C 46.98, H 6.87, N 8.22, Br 5.86. Found: C 47.05, H 6.55, N 8.23, Br 6.07.

Gadolinium(III)-1-(4-(2-(1-(4,7,10-triscarboxymethyl-(1,4,7,10-tetraazacyclododecyl)))ethylcarbamoyloxymethyl)-2-nitrophenyl)-β-D-glucopyronuronate (1). A quantity of 455 mg of **13** in 10 mL of water was cooled to 0 °C; 2.12 mL of 1 N NaOH was added over 1 min, and the solution was allowed to stir for 75 min. The pH was brought to 6.5 with 0.1 N HCl, and 216 mg of $GdCl_3$ (dissolved in 5 mL of water and brought to pH = 6.5 with NaOH) was added dropwise. The pH was kept above 5.5 during metal addition with 1 N NaOH. The solution was allowed to warm to room temperature while stirring, and the pH was adjusted periodically to keep it between 6 and 6.5. After 3 days at room temperature, the pH showed no change and the reaction was considered complete. The pH was brought to 8.2 and the solution centrifuged to remove excess gadolinium as $Gd(OH)_3$. Trace solids were removed by filtration through a 0.2 μm nylon filter, and the solution was lyophilized. The solid was brought up in 3 mL of water and purified on preparative HPLC using the following method: 0−10% B over 10 min, hold for 15 min at 10% B, then wash to 98% B before returning to 0% B. Two runs using this method were sufficient to give material that was pure by microanalysis. Yield: 185 mg **1** (17.7% from **10**). The compound was stored at −20 °C. Analysis of this material by analytic LC−MS (using the same method as in the preparative runs) gave a single peak in the PDA at 12.9 min with a m/z = 914.4 ($M - H^+$ ESI-MS) of appropriate isotope pattern. Calcd for $C_{30}H_{40}N_6O_{17}Gd$·2.5H_2O (87% Na^+ salt): C 37.85, H 4.46, N 8.83, Gd 16.52, Na 2.10. Found: C 37.69, H 4.28, N 9.12, Gd 16.88, Na 2.10.

Europium(III)-1-(4-(2-(1-(4,7,10-triscarboxymethyl-(1,4,7,10-tetraazacyclododecyl)))ethylcarbamoyloxymethyl)-2-nitrophenyl)-β-D-glucopyronuronate (4). This compound was synthesized and purified in the same manner as **1** using 168 mg of **13** and substituting $EuCl_3$ for $GdCl_3$. Yield: 70 mg of **4** (18.1% from **10**). The compound was stored at −20 °C. Analysis of this material by analytic LC−MS (using the same method as in the preparative runs) gave a single peak in the PDA at 12.9 min with a m/z = 907.2 ($M - H^+$ ESI-MS) of appropriate isotope pattern.

1-(2-^{t}Boc-aminoethyl)-(1,4,7,10-tetraazacyclododecane) (17). A quantity of 1.0 g (4.46 mmol) of 2-^{t}Boc-aminoethylbromide[30] was added to a stirring solution of 1.92 g (11.1 mmol) of cyclen in 60 mL of dry toluene. The solution was refluxed overnight under N_2 and extracted with 3 × 100 mL of water. The aqueous layer was extracted with 3 × 75 mL of CH_2Cl_2, and the combined CH_2Cl_2 extracts were dried over $MgSO_4$. Removal of solvent gave a white solid that was washed with cold Et_2O and dried in vacuo. This yielded 890 mg (63%) of **15**. ^{1}H NMR (500 MHz, $CDCl_3$): δ 1.44 (s, 9H), 2.59 (br s, 10H), 2.63 (br s, 4H), 2.82 (br s, 4H), 3.22 (br s, 2H); ^{13}C NMR (126 MHz, $CDCl_3$) δ 28.58, 38.65, 46.21, 47.28, 47.92, 52.20, 54.28, 78.96, 156.14; ESI-MS m/z $(M + H)^+$ 316.3. Anal. Calcd for $C_{15}H_{33}N_5O_2$: C 57.11, H 10.54, N 22.20. Found: C 57.43, H 10.47, N 22.51.

1-(2-^{t}Boc-aminoethyl)-4,7,10-(tris-^{t}butylcarboxymethyl)-(1,4,7,10-tetraazacyclododecane) (18). To a solution of 950 mg of **17** (3.01 mmol) and 3.29 g (31.0 mmol) of Na_2CO_3 in dry MeCN under N_2 was added 2.4 mL (15.1 mmol) of α-bromo-^{t}butyl acetate. The suspension was refluxed for 24 h, filtered, washed with 3 × 250 mL of hexanes, and concentrated in vacuo to give a yellow oil. The resulting oil was purified by chromatography (silica, 0−10% MeOH in CH_2Cl_2) to give 1.70 g (76%) of **18** as a white solid. Spectral and analytic data indicate a mixture of free base and HBr salt. The ^{1}H NMR was very broad between 2 and 3.8 ppm and therefore unasssignable.^{13}C NMR (126 MHz, $CDCl_3$): δ (major product) 27.73, 27.92, 28.03, 28.32, 37.69, 48.01, 49.88, 50.09, 52.50, 53.01, 53.82, 55.60, 56.40 (br), 56.91, 79.17, 81.70, 82.74, 156.40, 169.99, 172.51; (minor peaks): 79.30, 81.80, 82.36, 170.33, 173.28 (br); ESI-MS m/z $(M + H)^+$ 658.4 (60%), $(M + Na)^+$ 680.3 (100%). Anal. Calcd for $C_{33}H_{63}N_5O_8$·0.9HBr·H_2O: C 52.94, H 8.87, N 9.35, Br 9.60. Found: C 52.81, H 8.99, N 9.02, Br 9.78.

1-(2-Aminoethyl)-4,7,10-(triscarboxymethyl)-(1,4,7,10-tetraazacyclododecane) TFA Salt (19). Deprotection of 192 mg of **18** was achieved by stirring at room temperature in 4.75 mL of trifluoroacetic acid with 125 μL of both triisopropylsilane and water. After 17 h, the volatiles were removed in vacuo, and 40 mL of Et_2O was added to precipitate the ligand. The suspension was centrifuged and the white pellet washed with 3 × 50 mL of Et_2O. The resulting solid was dried under vacuum and yielded 135 mg of the TFA salt, **19**. ^{1}H NMR showed no remaining ^{t}butyl resonances, while ^{19}F NMR showed a signal for TFA. ESI-MS m/z $(M + H)^+$ 390.2.

Gadolinium(III)-1-(2-aminoethyl)-4,7,10-(triscarboxymethyl)-(1,4,7,10-tetraazacyclododecane) (2). A quantity of 128 mg (0.61 mmol) of $Gd(OH)_3$·H_2O and 239 mg of **19** were combined in 10 mL of water, and the suspension was refluxed for 48 h. The solution was brought to pH = 10 with concentrated NH_4OH and centrifuged to remove excess $Gd(OH)_3$. The pellet was washed, and the combined washings and supernatant were lyophilized. The resulting solid was dissolved in water and purified by successive runs on preparative HPLC using the following method: 0−20% B over 10 min, hold at 20% B for 15 min, then wash to 98% B before returning to 0% B. Due to the lack of chromophores, the compound displays little UV absorption;

(30) Sakai, N.; Gerard, D.; Matile, S. *J. Am. Chem. Soc.* **2001**, *123*, 2517−2524.

fluorescence, however, can be detected by exciting at 271 nm and monitoring the emission at 314 nm. Due to peak tailing, fractions were analyzed by analytic LC−MS, and those containing **2** were pooled and lyophilized; 101 mg of **2** was obtained analytically pure by this approach (40% from **18**). ESI-MS *m*/*z* $(M + Na)^+$ 567.0 with Gd isotope pattern. Anal. Calcd for $C_{16}H_{28}N_5O_6Gd\cdot H_2O$: C 34.21, H 5.38, N 12.47. Found: C 34.16, H 5.31, N 12.08.

Europium(III)-1-(2-aminoethyl)-4,7,10-(triscarboxymethyl)-(1,4,7,10-tetraazacyclododecane) (3). A quantity of 128 mg of **19** and 132 mg (0.36 mmol) of $EuCl_3\cdot 6H_2O$ were combined in water, and the pH was adjusted to 6 with 1 N NaOH. The reaction was stirred for 3 days at room temperature, filtered, and lyophilized. The freeze-dried solid was purified in the same manner (and exhibited similar peak tailing) as **2** except fluorescence detection used $\lambda_{ex} = 395$ nm and $\lambda_{em} = 615$ nm; 45 mg of **3** was obtained analytically pure in this fashion (33% from **18**). ESI-MS *m*/*z* $(M + Na)^+$ 559.8, 561.7, Eu isotope pattern. Anal. Calcd for $C_{16}H_{28}N_5O_6Eu\cdot 0.5H_2O$: C 35.11, H 5.34, N 12.79, Eu 27.76. Found: C 35.03, H 5.41, N 12.54, Eu 27.89.

Relaxivity. A 4 mM stock solution of either **1** or **2** in the appropriate buffer was diluted to give 500 μL of each of seven approximate concentrations for each run: 0, 0.05, 0.15, 0.3, 0.5, 1.0, and 2.0 mM. The T_1 of each concentration was determined using an inversion recovery pulse sequence with appropriate recycle delays on a Bruker mq60 Minispec. This instrument has a proton Larmor frequency of 60 MHz and operates at 37 °C. The resulting curves were fit to a monoexponential function to obtain T_1. Ten microliters of each sample was digested in concentrated nitric acid, diluted with water, and analyzed for exact Gd(III) concentration using ICP-MS. The reciprocal of the longitudinal relaxation time was plotted against the concentration obtained from ICP-MS and fit to a straight line. All lines were fit with $R^2 > 0.998$. This was performed for each buffer in duplicate. The buffers were all made to have the appropriate pH at 37 °C and remade if the pH had drifted more than 0.05 pH units upon storage. Anion mimic and carbonate-containing buffers were made fresh daily.

Enzyme Kinetics. Bovine liver β-glucuronidase (Type B-1, Sigma G 0251) stability in several buffers was assayed by the Sigma quality control assay for β-glucuronidase from bovine liver. It was determined that MOPS and anion mimic[31] engendered the enzyme with poor stability, while 100 mM phosphate with 0.01% (w/v) bovine serum albumin (BSA), pH = 7.4 at 37 °C, gave suitable stability (>2 h at 37 °C without loss of activity) provided the enzyme concentration was greater than 0.5 mg/mL. The enzyme was stable for at least 24 h at 37 °C at its native pH of 5.0 in 100 mM acetate buffer.

LC−MS. After incubating **1** (0.2 mM) with bovine liver β-glucuronidase (1 mg/mL) in the above phosphate buffer at 37 °C, the reaction mixture was analyzed by LC−MS and showed the presence of 4-hydroxy-3-nitrobenzyl alcohol at 4.0 min, substrate **1** at 7.5 min, and **2** at 11.8 min. The alcohol and **1** are readily distinguished by their absorption spectra (PDA), their appropriate negative mode ESI-MS patterns, and through spiking with authentic compound. **2** could be observed using fluorescence. The HPLC method was as follows: 0−10% B over 10 min, hold at 10% B for 15 min, with fluorescence using $\lambda_{ex} = 271$ nm and $\lambda_{em} = 314$ nm.

UV−Visible. The enzymatic hydrolysis of the pyranose from **1** and subsequent linker decomposition generates 4-hydroxy-3-nitrobenzyl alcohol. The molar absorptivity, ϵ, of this alcohol at 422 nm was determined in triplicate to be 2840 ± 40 M^{-1} cm^{-1} in 100 mM phosphate, 0.01% (w/v) BSA, pH = 7.4 at 37 °C. At pH = 7.4, the substrate, **1**, does not absorb at this wavelength. The kinetics were sampled on the HP 8452A at 37 °C every 5 s for 10 min. The initial velocities for pH = 7.4 buffers were determined through a linear fit of the first 10% change in absorbance. The Michaelis−Menten parameters for **1** were determined by plotting the initial velocity versus substrate concentration for concentrations ranging from 0.1 to 4.0 mM. The measurements were made in triplicate with 1.0 mg/mL enzyme in a 500 μL sample. Control experiments without enzyme or substrate showed negligible absorption over the time period of the experiment. Fitting of the resulting data was performed using Origin 7.0. Analysis of the reaction mixture by LC−MS using the method detailed in purification of **1** after 10 min confirmed the presence of 4-hydroxy-3-nitrobenzyl alcohol and compound **2**. The ϵ of *p*-nitrophenol at 422 nm was determined to be 7660 ± 180 M^{-1} cm^{-1} in the same fashion as 4-hydroxy-3-nitrobenzyl alcohol. The determination of K_m and V_{max} for *p*-nitrophenyl-β-D-glucuronide was performed in the same manner as for **1** except the substrate concentrations were varied from 0.5 to 30.0 mM.

Magnetic Resonance. Samples consisting of 0.2 mM **1** and 1.0 mg/mL of enzyme in 500 μL of phosphate buffer were monitored by UV−visible and magnetic resonance. T_1 was determined using a saturation recovery (90−τ−90) pulse sequence on the Bruker mq60 operating as detailed in the relaxivity section. The runs were performed in triplicate. The substrate-only control was also examined in this manner. The enzyme-only controls showed T_1's that were identical to neat buffer. In all instances, with the exception of the magnetic resonance substrate control in acetate buffer, the controls showed very little change over the 1 h duration of each experiment. The substrate in acetate buffer showed a slight (2%) decrease in T_1 over the course of an hour. This trend is in the opposite direction of the kinetics runs that show an increase in T_1.

Determination of *q*. Europium(III) compound **4** was dissolved in H_2O and D_2O. The emission was monitored at 614 nm with excitation at 394 nm on a Hitachi F4500 fluorometer operating in phosphorescence lifetime (short) mode. The shortest lifetime measurable with this instrument is about 0.3 ms. Fifteen scans were averaged and fit to a monoexponential decay to give phosphorescent lifetimes: τ (D_2O) = 1.274 ms; τ (H_2O) = 0.527 ms at room temperature. Using the equation of Supkowski and Horrocks,[32a] $q = 0.89$ (correction for a single N−H amide-like oscillator gives $q = 0.81$), while the equation from Beeby et al.[32b] generates $q = 1.0$ (N−H correction gives $q = 0.95$). At 37 °C, τ (D_2O) = 1.197 ms; τ (H_2O) = 0.458 ms. Supkowski and Horrocks give $q = 1.2$ (correction for a single N−H amide-like oscillator gives $q = 1.1$). Using the equation from Beeby et al., $q = 1.3$ (N−H correction gives $q = 1.2$).

Synthesis

The synthesis of **1** begins with methyl 1-bromo-2,3,4-tri-*O*-acetyl-α-D-glucopyronuronate[33] (Scheme 2). Coupling of 4-hydroxy-3-nitrobenzaldehyde to the pyranose via a Koenigs−Knorr reaction followed by sodium borohydride reduction produced **7** in 92% yield without recourse to chromatography. Initial attempts at formation of the carbamate using *p*-nitrophenyl chloroformate[34,35] and triphosgene[36,37] gave intermediates that showed insufficient reactivity toward 2-bromoethylamine and 2-hydroxyethylamine. The reaction occurred smoothly, however, when carbonyldiimidazole (CDI) was used as the carbonyl equivalent. Methylation of the monoimidazolyl intermediate gave an increased yield through precipitation of the cationic intermediate.

Alkylation reactions involving **9** with either cyclen or DO3A(tris-^{t}butyl ester)[38] generated large amounts of α,β-

(31) Parker, D. In *Crown Compounds: Towards Future Applications*; Cooper, S. R., Ed.; VCH: New York, 1992; pp 51−67.
(32) (a) Supkowski, R. M.; Horrocks, W. D., Jr. *Inorg. Chim. Acta* **2002**, *340*, 44−48. (b) Beeby, A.; Clarkson, I. M.; Dickins, R. S.; Faulkner, S.; Parker, D.; Royle, L.; de Sousa, A. S.; Williams, J. A. G.; Woods, M. *J. Chem. Soc., Perkin Trans. 2* **1999**, 493−504.
(33) Bollenback, G. N.; Long, J. W.; Benjamin, D. G.; Lindquist, J. A. *J. Am. Chem. Soc.* **1955**, *77*, 3310−3315.
(34) Florent, J.-C. et al. *J. Med. Chem.* **1998**, *41*, 3572−3581.
(35) Leu, Y. L.; Roffler, S. R.; Chern, J. W. *J. Med. Chem.* **1999**, *42*, 3623−3628.
(36) Eckert, H.; Forster, B. *Angew. Chem.* **1987**, *99*, 922−923.
(37) Majer, P.; Randad, R. S. *J. Org. Chem.* **1994**, *59*, 1937−1938.

Scheme 2

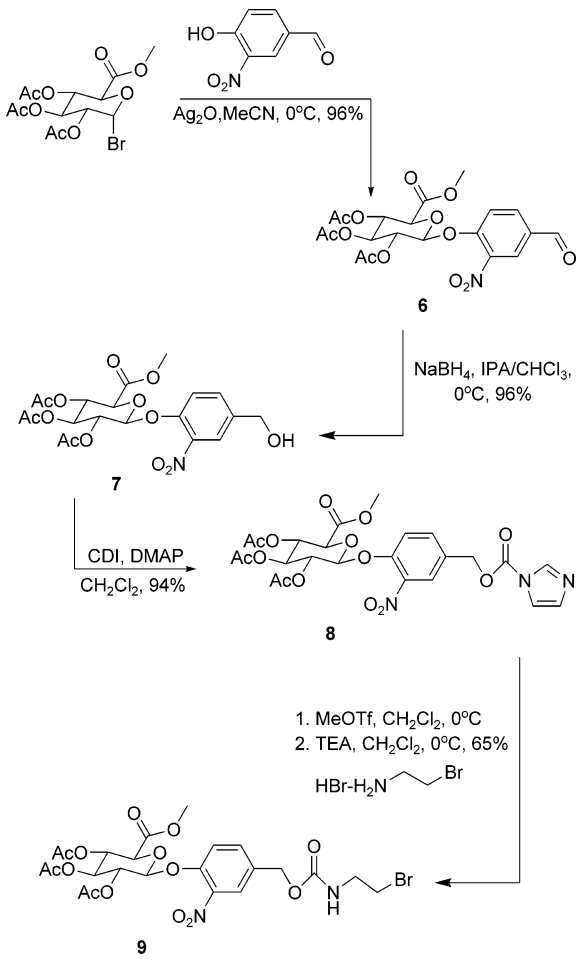

Scheme 3

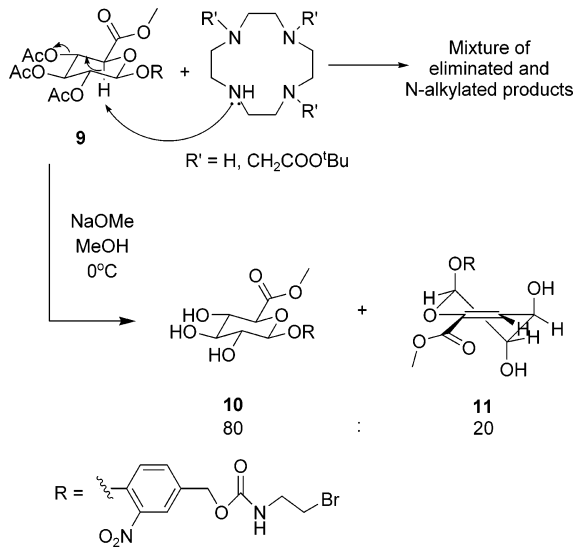

unsaturated byproducts due to an acid−base reaction between cyclen and the acidic proton α to the methyl ester (Scheme 3). It is known that this type of elimination can happen with acetyl-protected glucuronic acids,[39,40] but it is rarely mentioned in the literature. Synthesis of methyl-1-ethoxy-2,3,4-tri-*O*-acetyl-β-D-glucopyronuronate and subsequent monitoring of the reaction

(38) Dadabhoy, A.; Faulkner, S.; Sammes, P. G. *J. Chem. Soc., Perkin Trans. 2* **2002**, 348−357.

Scheme 4 [a]

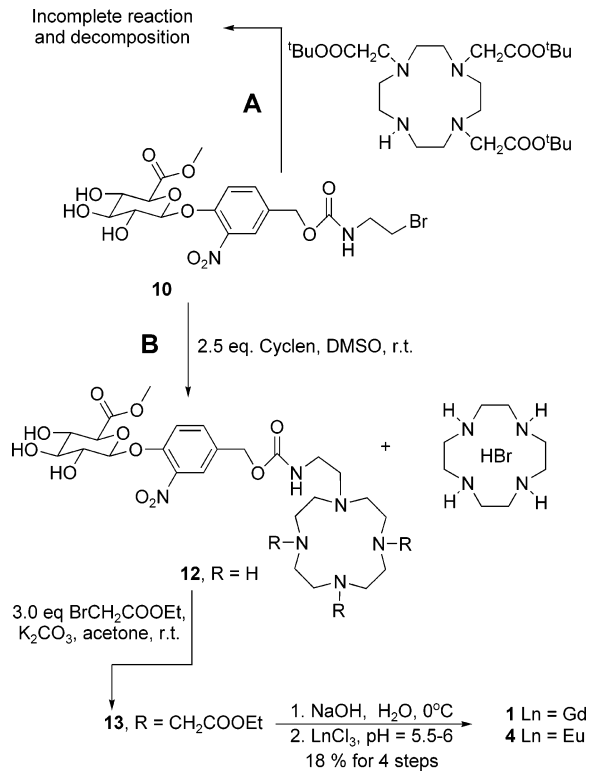

[a] Coupling of macrocycle to **10**, via DO3A route (A) or cyclen route (B).

with cyclen by ^{1}H NMR confirmed the elimination.[41] The formation of the α,β-unsaturated byproducts was circumvented by selective removal, in good yield, of the acetyl groups from **9** using sodium methoxide, with **11** as the byproduct (Scheme 3). Introduction of the macrocycle was then attempted through two approaches.

In the first approach, DO3A(tris-^{t}butyl ester) was reacted with **10** (Scheme 4, A). After several days at room temperature, the reaction was not complete and byproducts had begun to develop. Heating the reaction induced sugar decomposition. The cyclen route, in which the sugar-containing arm is added prior to the acetate arms (Scheme 4, B), was successful, presumably because the macrocycle free base is more nucleophilic toward the unactivated alkyl bromide electrophile than is the DO3A compound. Increasing the electrophilicity of **9** (Scheme 2) by making the mesylated compound, **14** from **8** (Scheme S1), was not successful due to the propensity of **14** to cyclize via elimination of the mesyl group in the presence of cyclen.

Purification of **12** proved difficult, so the compound was alkylated with ethyl bromoacetate. Excess cyclen, as the perethyl DOTA ester, could then be removed by chromatography on silica. Final deprotection and metalation were performed in a one-pot procedure. Compound **1** was obtained analytically pure, showing one peak by LC−MS with the appropriate isotope pattern after purification by preparative HPLC. The overall yield for the nine-step procedure was 8.0%. Compound **4** was obtained in 8.2% overall yield by substituting $EuCl_3$ for $GdCl_3$.

(39) Schmidt, H. W. H.; Neukom, H. *Tetrahedron Lett.* **1969**, 2011−2012.
(40) Stachulski, A. V.; Jenkins, G. N. *Nat. Prod. Rep.* **1998**, *15*, 173−186.
(41) Duimstra, J. A. *Carbohydrate-Based Gadolinium(III) Magnetic Resonance Imaging Contrast Agents: A Synthetic Retrospective.* M.S. Thesis, California Institute of Technology, Pasadena, 2002.

Scheme 5

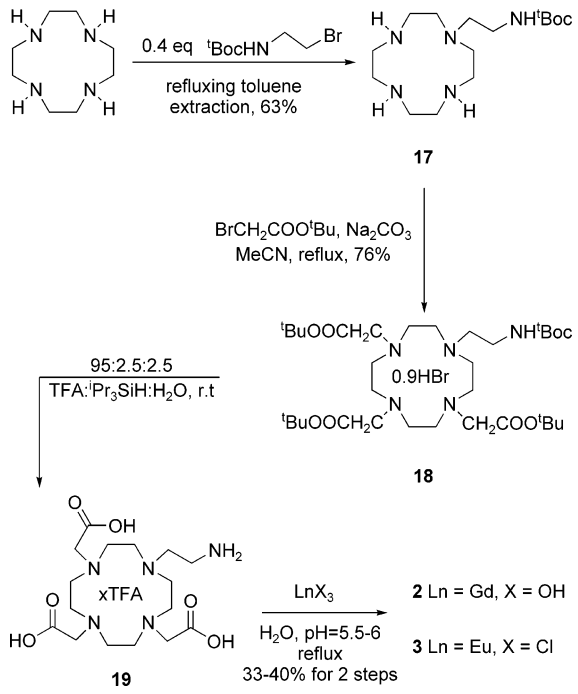

The synthesis of compounds **2** and **3** proved to be more straightforward (Scheme 5). Utilizing the monoalkylation of excess cyclen, intermediate **17** was obtained analytically pure following extraction and an ether wash. Subsequent alkylation with 3 equiv of *t*butyl bromoacetate gave **18** as a 9:1 mixture of hydrobromide salt to free base. Deprotection was achieved through the use of trifluoroacetic acid. Metalation of the free ligand, **19**, with $Gd(OH)_3$ gave crude **2**. Purification of **2** via HPLC was difficult for two reasons. The lack of a chromophore on **2** limited detection to fluorescence, and the presence of the primary amine ligand gave a peak with a long tail. These difficulties lowered the overall yield to 19% for four steps. The Eu(III) compound **3** was obtained in 16% overall yield by substituting $EuCl_3$ for $Gd(OH)_3$. Both compounds were determined to be authentic by elemental analysis.

Relaxivity

The defining parameter of contrast agent efficacy is relaxivity. In this context, relaxivity, r_1, is a measure of the extent to which the agent, per unit, catalyzes the shortening of the longitudinal relaxation time, T_1, of protons on the hydrogen atoms in bulk water. The presence of other species in solution, be they salts, proteins, or small molecules, can have a marked effect on an agent's relaxivity. Relaxivity measurements made in solutions of varying composition not only describe how the agent responds to that composition but also provide insight into the microscopic processes occurring at or near the Gd(III) center. Attributing relaxivity effects to solution composition can only be made when the contrast agent under study is of a known purity. The use of analytically pure contrast agents allows for facile and accurate determination of agent concentration through the use of Gd(III) ICP-MS. This, in tandem with measurements made in duplicate, reduces the systematic error in the relaxivity measurements.

The measurements shown in Figure 1 reveal trends in relaxivity related to buffer composition. To provide a reference, the relaxivity of the known $q = 1$ contrast agent (q is the number

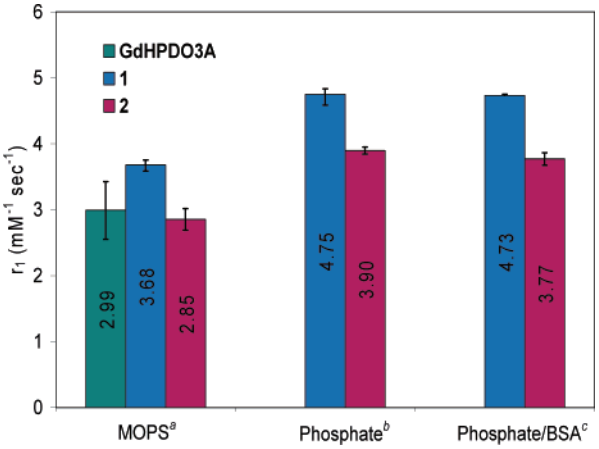

Figure 1. T_1 relaxivity of GdHPDO3A, **1**, and **2** at 60 MHz, 37 °C, pH = 7.4. Error is ±1 standard deviation of duplicate measurements: [a]10 mM MOPS, 100 mM NaCl; [b]100 mM sodium phosphate; [c]100 mM sodium phosphate, 0.01% (w/v) bovine serum albumin (BSA).

of water molecules coordinated to the metal center), Gd(III)-2-hydroxypropyl-DO3A (GdHP-DO3A) was measured in pH = 7.4 MOPS buffer and gave an $r_1 = 2.99 \pm 0.44$ mM^{-1} s^{-1} under these conditions. It has been reported that MOPS does not coordinate to the metal center. Bretonniere and coworkers[42,43] performed experiments in MOPS without interference with carbonate binding to Eu(III) trisamide cyclen complexes, while Bruce et al.[44] indicate that experiments with related compounds may be run in the structurally similar HEPES. Initial relaxivity measurements of **1** and **2** made in the same MOPS buffer showed a higher value for **1** and a value comparable to GdHP-DO3A for **2** (Figure 1, MOPS columns). The magnitude of r_1 for **1** is somewhat low for a $q = 2$ complex,[45] indicating intramolecular coordination of the sugar-containing arm to the metal center. Determination of q at room temperature via Eu(III) fluorescence[32] for **4** (the Eu(III) analogue of **1**) in the absence of buffer salts gave a $q = 1$, supporting the intramolecular coordination postulate. Presumably, this coordination occurs through the carbamate carbonyl oxygen. A similar seven-membered intramolecular ring has been invoked to explain low q values for EuDO3A-type complexes containing tethered carboxylates.[46,47] The donating ability of a carbamate carbonyl oxygen is expected to be lower than that of a carboxylate due to increased electron density delocalization and charge neutrality. This does not, however, preclude weak binding of the carbamate moiety to the metal center in **1**, giving a species that has one inner-sphere water molecule. Measurement of q at 37 °C supports this postulate. Here, the q is slightly higher with a value of 1.1−1.2, a result which indicates a weakening of the interaction between carbamate and metal center.[48]

Due to enzyme instability in MOPS buffer, the relaxivities of **1** and **2** were determined in the enzyme kinetics buffer composed of phosphate and BSA (Figure 1). Here, the relax-

(42) Bretonniere, Y.; Cann, M. J.; Parker, D.; Slater, R. *Chem. Commun.* **2002**, 1930−1931.
(43) Bretonniere, Y.; Cann, M. J.; Parker, D.; Slater, R. *Org. Biomol. Chem.* **2004**, *2*, 1624−1632.
(44) Bruce, J. I. et al. *J. Am. Chem. Soc.* **2000**, *122*, 9674−9684.
(45) Since r_1 is directly proportional to q (see ref 13), a $q = 2$ complex should show an r_1 approximately twice that of a $q = 1$ complex, such as GdHP-DO3A
(46) Messeri, D.; Lowe, M. P.; Parker, D.; Botta, M. *Chem. Commun.* **2001**, 2742−2743.
(47) Lowe, M. P.; Parker, D.; Reany, O.; Aime, S.; Botta, M.; Castellano, G.; Gianolio, E.; Pagliarin, R. *J. Am. Chem. Soc.* **2001**, *123*, 7601−7609.

ivities are higher (4.73 vs 3.68 mM^{-1} s^{-1}) but show the same trend as observed in MOPS buffer, namely, a 20% drop in relaxivity upon going from **1** to **2**. In this case, however, it is unclear if the species in solution is an intramolecularly coordinated **1** or a ternary adduct in which phosphate has displaced carbamate binding. Phosphate is known to coordinate to DO3A analogues in a monodentate fashion[44,49−52] and could, therefore, compete with intramolecular coordination, especially at the relatively high concentrations employed here.

The native lysosomal environment of β-glucuronidase is acidic, with maximum activity observed between pH = 4−5.[53] The relaxivity of compounds **1** and **2** was thus measured at pH = 5.0. The results from two different buffers at the same pH are dramatically different. In 10 mM pyridine, 100 mM sodium chloride buffer, compound **1** has a relaxivity of 3.89 ± 0.05 mM^{-1} s^{-1}, while **2** displays an r_1 of 4.16 ± 0.09 mM^{-1} s^{-1}. In 100 mM acetate buffer, those values are 2.53 ± 0.01 and 2.16 ± 0.04 mM^{-1} s^{-1}, respectively. The difference between buffers may be due to the coordinating ability of the buffer constituents. Pyridine is expected to be a poor ligand for the oxophilic Gd(III) in water[54] and thus does not restrict water access to the metal center as much as acetate. At pH = 7, propionate binding to GdDO3A has been shown to be monodentate,[55] and TbDO3A, in the presence of a large excess of acetate, gives a q value of 1.[44] To our knowledge, the coordination of acetate or pyridine to LnDO3A and its analogues has not been examined at pH = 5.0.

Our studies on EGad and EGadMe demonstrate that in vitro measurements do not correlate with in vivo efficacy. While an MR contrast agent may display efficacy in vitro, the addition of the components found in blood plasma could result in a significant change in the properties of the agent. To investigate these effects and the interplay of coordinating bidentate anions on the present β-glucuronidase-sensitive agent, we measured the relaxivity of **1** and **2** in buffers of increasing compositional complexity. These results are depicted in Figure 2. For the MOPS and phosphate data, the effects are superimposed upon the overall relaxivity differences observed between the two buffers (Figure 1). Addition of physiologically relevant carbonate concentrations (24 mM)[31] to the buffers displayed in Figure 1 gave similar results independent of buffer; namely, the relaxivity of **1** decreased by 20−30%, while that of **2** remained the same within error. These data support our initial hypothesis of stronger binding of carbonate to **1** versus **2** and would indicate that carbonate binding can displace the seven-membered carbamate chelate. Results with the anion extracellular mimic[31,44] continue the trend begun in the carbonate-containing buffers. Here, the data exhibit the desired dark to bright (lower to higher

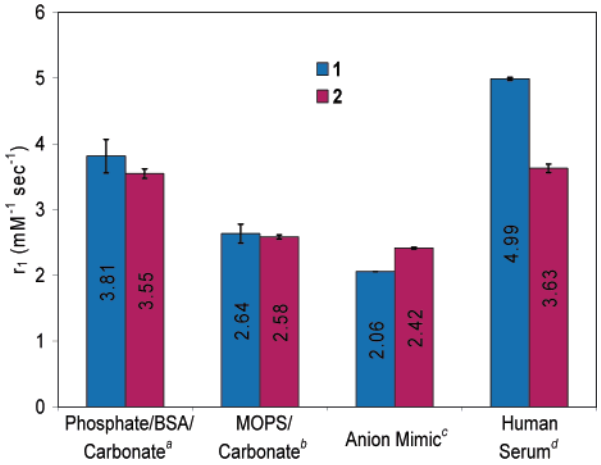

Figure 2. T_1 relaxivity of **1** and **2** at 60 MHz, 37 °C, pH = 7.4. Error is ±1 standard deviation of duplicate measurements: [a]100 mM sodium phosphate, 0.01% (w/v) BSA, 24 mM $NaHCO_3$; [b]10 mM MOPS, 24 mM $NaHCO_3$; [c]100 mM NaCl, 0.9 mM Na_2HPO_4, 30 mM $NaHCO_3$, 0.13 mM sodium citrate, 2.3 mM sodium lactate;[44] [d]male human blood serum.

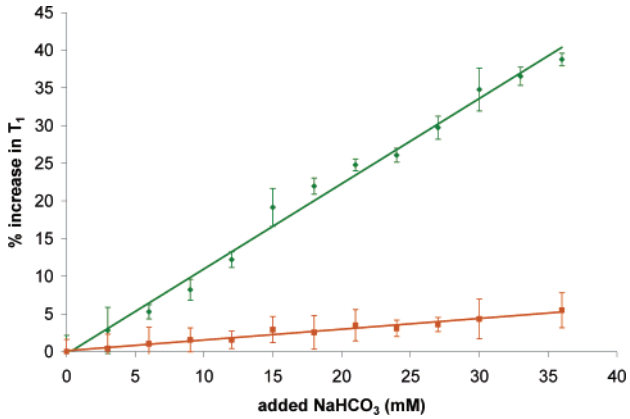

Figure 3. Change in T_1 of **1** (green ◆) and **2** (orange ■) as a function of added sodium bicarbonate: 0.5 mM complex, 100 mM MOPS, 60 MHz, 37 °C, pH = 7.4. Error is ±1 standard deviation of duplicate measurements. Lines are best linear least-squares fit to data.

relaxivity) change. In this case, it is a 17% increase. Once again, the decrease is more dramatic for **1** (22%) than for **2** (6%), providing more evidence for the increased chelating anion affinity of **1** compared to that of **2**.

Carbonate is known to bind seven-coordinate cis-divacant LnDO3A analogues more strongly than to eight-coordinate LnDOTA analogues.[44,46,50,51] The relaxivities of **1** and **2** (Figure 2) follow this trend. Figure 3 displays the change in T_1 observed upon titration of these agents with sodium bicarbonate in a physiologically relevant range at pH = 7.4. **2** has a small dependence on added bicarbonate (0.14% increase in T_1 per mM bicarbonate) in this range, while **1** displays a stronger correlation at 1.1% increase in T_1 per mM bicarbonate,[56] indicating displacement of intramolecular carbamate coordination. The results correlate well with the change in relaxivity of the two compounds upon addition of 24 mM bicarbonate (Figures 1 and 2). The titration of **1** has not begun to saturate at 36 mM added bicarbonate, indicative of a small binding constant for the ternary complex. This result contrasts sharply with the results observed for the tri-positive Ln(III) tris amide cyclen complexes. These

(48) The q values at elevated temperatures must be viewed with caution since the empirically observed relationship between phosphorescence lifetime and coordination number was evaluated at room temperature. It is unlikely that the empirical parameters will be independent of temperature.
(49) Aime, S.; Gianolio, E.; Terreno, E.; Giovenzana, G. B.; Pagliarin, R.; Sisti, M.; Palmisano, G.; Botta, M.; Lowe, M. P.; Parker, D. *J. Biol. Inorg. Chem.* **2000**, *5*, 488−497.
(50) Dickins, R. S. et al. *J. Am. Chem. Soc.* **2002**, *124*, 12697−12705.
(51) Supkowski, R. M.; Horrocks, W. D., Jr. *Inorg. Chem.* **1999**, *38*, 5616−5619.
(52) Vander Elst, L.; Van Haverbeke, Y.; Goudemant, J. F.; Muller, R. N. *Magn. Reson. Med.* **1994**, *31*, 437−444.
(53) Himeno, M.; Hashiguchi, Y.; Kato, K. *J. Biochem. (Tokyo)* **1974**, *76*, 1243−1252.
(54) A search of the CSD returned no structures containing a lanthanide coordinated to both a pyridyl and aquo ligand.
(55) Aime, S.; Terreno, E.; Botta, M.; Bruce, J. I.; Parker, D.; Mainero, V. *Chem. Commun.* **2001**, 115−116.
(56) The concentration of the various carbonate species is a function of pH, as discussed in Bruce et al.[44]

complexes display saturation with as little as 2 mM added bicarbonate.[44] The lower affinity for carbonate species of complex **1** compared to that of the tris amide complexes can be attributed to the lower charge (neutral versus 3^+) and the binding competition with the intramolecular carbamate chelation.

If the coordination of endogenous anions was the sole intermolecular contributor to the relaxivities observed in these contrast agents, then results from the anion extracellular mimic would translate well to results obtained in human blood serum. The present case shows the dramatic differences on going from a competitive extracellular anion mimic to human serum. The data are entirely different as compound **1** shows an increase in relaxivity of 240%, while compound **2** displays a 150% increase. Furthermore, the relaxivity differential has switched with **1** 27% brighter than **2** in serum. On the basis of our previous work, this difference should be sufficient for in vivo imaging.[25] For these compounds in serum, the relaxivity indicates a species containing inner-sphere water molecules, in contrast to the $q = 0$ species detected by Aime et al. for DO3A analogues in the presence of albumin.[49] The complex composition of human serum makes it difficult to ascribe the results to any given component, but the higher viscosity and possible macromolecular interactions could affect τ_R and hence the relaxivity.

Enzyme Kinetics

To study the enzymatic processing of **1**, we chose to use β-glucuronidase isolated from bovine liver. This commercially available enzyme is more similar to the human variant than the *E. coli* version.[57,58] The bovine liver enzyme is localized in the lysosome and hence has maximal activity at pH = 5.[53] At neutral interstitial pH, the activity of both the human and bovine liver enzymes is 10% that at pH = 5 and falls off rapidly in more alkaline solutions.[53,59] The attenuation of activity is significant since ADEPT and PMT function at interstitial pH. The lower pH around tumor masses is advantageous in this respect as enzyme activity will be higher. Although the bacterial enzyme has much higher activity at extracellular pH,[60] it is obviously not endogenous to humans and its use in ADEPT has resulted in host immune response[16,18] severely restricting its potential. Furthermore, the 2-nitroquinonemethide that results from enzymatic processing of **1** is not an irreversible inhibitor of bovine β-glucuronidase.[57]

LC−MS provided a facile means to detect and identify the components of the enzyme-catalyzed hydrolysis of **1**. After a 2 h reaction in phosphate buffer, the presence of 4-hydroxy-3-nitrobenzyl alcohol could be easily detected in the LC data at 4.0 min; unreacted **1** was observed at 7.5 min, and **2** appeared at 11.8 min. **1** had disappeared after 24 h. The verification of the presence of 4-hydroxy-3-nitrobenzyl alcohol enabled the enzyme kinetics in phosphate/BSA buffer to be quantified using a continuous UV−visible assay.[61] The alcohol has an absorption maximum at 422 nm, while **1** does not absorb at this wavelength. A plot of initial velocity versus substrate concentration fits well to a single-site Michaelis−Menten model (Figure 4). The kinetic

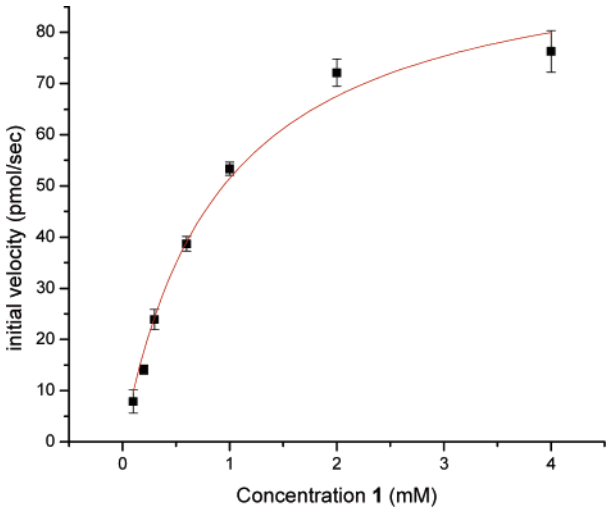

Figure 4. Kinetics of hydrolysis of **1** catalyzed by bovine liver β-glucuronidase. Each point is the average of three runs ±1 standard deviation. Line represents best fit to Michaelis−Menten model. Conditions are 1.0 mg/mL of enzyme in 100 mM sodium phosphate, 0.01% (w/v) bovine serum albumin (BSA), pH = 7.4 at 37 °C.

Table 1. Enzyme Kinetic Parameters for **1** and PNG

substrate	pH[a]	K_m (mM)	V_{max} (pmol s^{-1})	k_{cat}/K_m (M^{-1} s^{-1})
1[b]	7.4	0.906 ±0.133	98 ± 5.5	74.0 ± 10.9
PNG[b]	7.4	18.5 ± 5.6	184 ± 30	6.76 ± 2.05
PNG[c]	5	0.33		
PNG[d]	7.2	1.40 ± 0.42		47

[a] At 37 °C. [b] With 1.0 mg/mL of bovine liver β-glucuronidase (type B-1), 100 mM sodium phosphate, 0.01% (w/v) bovine serum albumin (BSA). Data are average of three runs ± 1 standard deviation. [c] Bovine liver β-glucuronidase.[53] [d] Human recombinant β-glucuronidase.[62]

parameters from the nonlinear fit are tabulated in Table 1. For comparison, k_{cat}/K_m was determined for the standard assay substrate, *p*-nitrophenyl-β-D-glucuronide (PNG). The data obtained show that **1** is a better substrate by an order of magnitude for bovine liver β-glucuronidase than is PNG (Table 1). These kinetics demonstrate the marked improvement afforded by incorporation of the self-immolative linker. The nonimmolative β-galactosidase-sensitive agent, EGadMe, displayed enzyme kinetics that were 2−3 orders of magnitude worse than that of the standard β-galactosidase substrate, 2-nitrophenyl-β-D-galactopyranoside.[25]

The kinetics can also be monitored using magnetic resonance. The use of MR allowed observation of kinetics in human serum, something that could not be done by visible light spectroscopy due to light scatter by suspended particles. Figure 5 shows the normalized change in T_1 as a function of enzyme incubation time. The results show excellent correlation with the relaxivities of the substrate **1** and the product **2**, measured in the absence of enzyme (Figures 1 and 2). The largest change detected for the pH = 7.4 buffers comes from the data in human serum. Here, a 14% increase is observed over the course of 1 h, and the curve has not saturated at this time. The control without enzyme maintains a constant T_1 over this period. These serum experiments demonstrate that the contrast agent functions well in the complex biological milieu represented by human serum.

(57) Azoulay, M.; Chalard, F.; Gesson, J. P.; Florent, J. C.; Monneret, C. *Carbohydr. Res.* **2001**, *332*, 151−156.
(58) Brot, F. E.; Bell, C. E., Jr.; Sly, W. S. *Biochemistry* **1978**, *17*, 385−391.
(59) Jain, S.; Drendel, W. B.; Chen, Z.-w.; Mathews, F. S.; Sly, W. S.; Grubb, J. H. *Nat. Struct. Biol.* **1996**, *3*, 375−381.
(60) Jefferson, R. A.; Burgess, S. M.; Hirsh, D. *Proc. Natl. Acad. Sci. U.S.A.* **1986**, *83*, 8447−8451.
(61) Aich, S.; Delbaere, L. T. J.; Chen, R. *BioTechniques* **2001**, *30*, 846−850.
(62) O'Leary, K. A.; Day, A. J.; Needs, P. W.; Sly, W. S.; O'Brien, N. M.; Williamson, G. *FEBS Lett.* **2001**, *503*, 103−106.

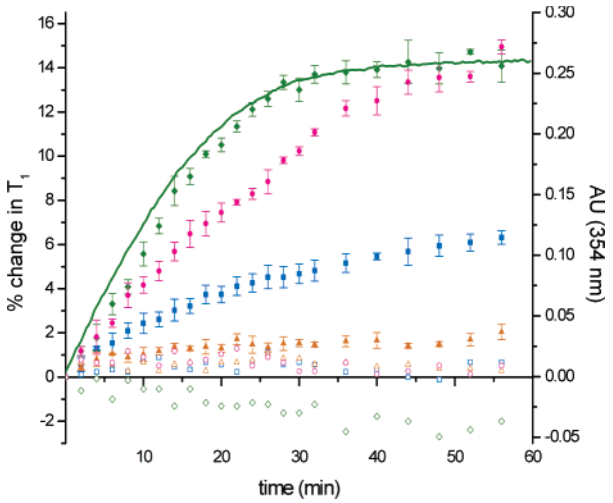

Figure 5. Kinetics of enzyme-catalyzed hydrolysis of **1** monitored by bulk water T_1 relaxation (60 MHz, 37 °C). Error bars on data (filled symbols) are ±1 standard deviation of three independent measurements. Open symbols are control runs without enzyme: (blue ■) 0.2 mM **1**, 1.0 mg/mL of β-glucuronidase, 100 mM sodium phosphate, 0.01% (w/v) bovine serum albumin (BSA), pH = 7.4; (orange ▲) 0.2 mM **1**, 1.0 mg/mL of β-glucuronidase, 100 mM sodium phosphate, 0.01% (w/v) bovine serum albumin (BSA), 24 mM $NaHCO_3$, pH = 7.4. Green line is hydrolysis of **1** monitored by UV−visible at 354 nm, conditions as for: (green ◆) 0.2 mM **1**, 0.1 mg/mL of β-glucuronidase, 100 mM sodium acetate, pH = 5.0; (red ●) 0.2 mM **1**, 1.0 mg/mL of β-glucuronidase, male human blood serum.

Enzyme instability precluded determination at long reaction times, but the shapes of the curves match those obtained from the UV−visible assays, indicating that compound **2** forms on a time scale similar to the change in absorbance of the aromatic linker. In particular, the longitudinal relaxation time observed in acetate buffer levels off at +15% around 35 min, corroborating well with both the complete conversion detected by absorption spectroscopy (solid line in Figure 5) and the 15% decrease in relaxivity observed between the pure compounds in acetate buffer.

The successful synthesis of an MRI contrast agent sensitive to the oncologically relevant enzyme β-glucuronidase expands the repertoire of agents responsive to biochemical reactions into the realm of clinically important processes. The relaxivity and kinetic assays developed in the present work elucidate the marked dependence that buffer composition can have upon the efficacy of an MR agent. Affinity for anions, such as carbonate, may be improved by increasing the electrostatic charge at the metal center through the replacement of anionic carboxylate ligands with neutral amide coordinating groups. The viability of the self-immolative linker conjugated to the macrocycle provides a model for future agents in which water access to the Gd(III) ion is restricted by a bridge connecting opposite sides of the macrocycle. Cleavage of a pendant moiety results in a cascade reaction that liberates the bridge, allowing water to access the inner-sphere coordination site. This class of agent in which inner-sphere coordination is blocked intramolecularly should function independently of endogenous anions.

Acknowledgment. This paper is dedicated in memory of Lorenzo J. Ponza. We thank Profs. Scott E. Fraser and Harry B. Gray for helpful discussions. Assistance with ICP-MS was provided by Keith MacRenaris. This work was supported by DOD Grant DAMD 17-02-1-0693 and NIH Grant 5 RO1 A147003.

Supporting Information Available: Synthesis of compounds **6**−**10** and **14**−**16** and complete refs 21, 34, 44, 50. This material is available free of charge via the Internet at http://pubs.acs.org.

JA042162R